Journal of Civil Engineering
The Institution of Engineers, Bangladesh
Vol. CE 29, No. 1, 2001

THREE DIMENSIONAL FINITE ELEMENT ANALYSIS OF A ROLLER COMPACTED CONCRETE (RCC) DAM DUE TO VARIABLE THERMAL LOADS

Ashna Nehrin[1] and Koichi Fujii[2]

ABSTRACT: In mass concrete such as in dams the temperature conditions are non-uniform. Consequently thermal stresses are developed even in the absence of external constraint solely because of the incompatibility of the natural expansions or contractions of the different parts of the dam. This paper focuses on the computer aided three-dimensional finite element transient thermal analysis during dry reservoir conditions, at different construction phases of a Roller Compacted Concrete (RCC) dam known as Hinata dam built at the Iwate Prefecture in Japan. It is important to predict the stress level due to temperature gradient in the accurate design of RCC dams considering the aspects of the maximum stress limitation of concrete and the durability of construction. The use of three-dimensional approach provides this paper with some distinction. This paper, therefore, aim at portraying the temperature and stress levels, incurred as the temperature varies over time, from the viewpoint of structural fracture. The results of this study are compared with the limits obtained by laboratory procedures during construction and can be used for prediction for RCC dams.

KEY WORDS: Roller Compacted Concrete (RCC), Dam. Temperature, Thermal Stress, Finite Element Analysis.

INTRODUCTION

Current technological trend requires the use of Roller Compacted Concrete (RCC) dams in order to overcome the risk of failure due to overtopping or internal erosion (piping) and to be economically competitive. The main difference between RCC and conventional concrete is its low cement content and no-slump consistency. It has been observed that there was a savings of about 30% for the construction of Hinata dam (Fig. 1) as compared to the cost of conventional concrete dams. The dam was constructed by

[1] Department of Agricultural Engineering, The United Graduate School of Agricultural Science, Iwate University, Morioka 020-8550, Japan
[2] Department of Agricultural Engineering, Faculty of Agriculture, Iwate University, Morioka, 020-8550, Japan.

placing RCC layers one above the other. Every new layer was made by spreading fresh RCC and then by compacting with vibratory rollers. Proper intervals between the placements were allowed in order to liberate as much heat of hydration as possible to the ambient. The construction of Hinata dam was undertaken in a temperate weather. Consequently, the speed of placements was more because of rapid heat loss to the ambient from exposed top surfaces. Portland cement liberated greater heat of hydration during hardening process. On the other hand, liberating smaller amount of heat hardened fly ash pozzolan. The fly ash pozzolan in RCC of Hinata dam constituted about 35% of total Portland cement content. This resulted in considerably lower heat of hydration generated from early age RCC, up to three times smaller than that of conventional concretes. The temperature rise occurred during the first days of placements when the creep effects were significant and the stiffness of RCC was still low. Therefore, the stresses developed at the early days were moderate and mainly compressive. After a few months, the stiffness had increased as the temperature dropped by interacting with the ambient. Consequently, relatively important thermally induced tensile stresses were developed, and thus thermal cracks would develop. During construction of the dam, our objective was to keep the temperature gradient as low as possible to avoid thermally induced cracks. The advantages of layer-wise construction for controlling the thermal stress were due to the use of thin layers that allowed greater surface of exposure for heat losses by convection to attain equal maturity level in terms of temperature. The time intervals between placing were kept almost constant that led to constant placing speed. This regularity at the time of construction produced smooth temperature gradients inside dam body. For large RCC dams such as the Hinata dam, it was essential to establish a construction programme which included the determination of lift schedule keeping some important factors in mind, viz. RCC mix composition, ambient temperature, placing temperature, layer thickness, and placing interval.

Generally the potential for cracking in RCC dams is unique to each site and depends on the heat rise within the mass, the ambient temperature, the thermoplastic and strength characteristics of RCC, and the geometric configuration of the dam section. Due to the massive structure of Hinata dam, the volume changes due to the temperature gradients were not continuous over the whole mass. The lower water content in RCC mixture led to less shrinkage.

Recent enhancement on finite element solution methodology has shown considerable power and versatility in case of heat transfer problems. The equations governing the heat conduction and thermoplastic problems are difficult to solve analytically, especially for the present three-dimensional case. Hence a finite element approach was preferred in this analysis. The finite element

represented an approximate numerical solution of a boundary value problem described by a differential equation. The thermal module of the FEA computer program (ANSYS 5.5.3) was used for the solution process.

Fig 1(a). Photograph of Hinata Dam

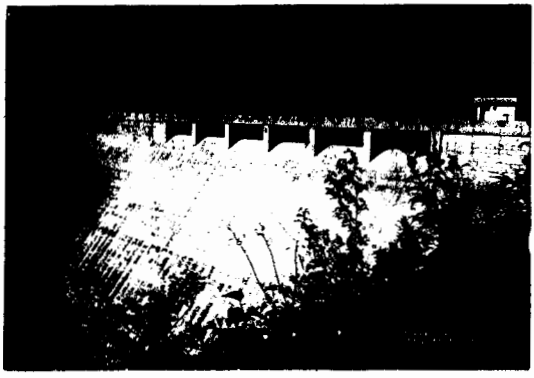

Fig 1(b). Photograph of Hinata Dam

LITERATURE REVIEW

Since the first RCC dams, Shimajigawa, Japan, in 1980 and Willow Creek, USA, in 1982, were built, there has been a steady increase in the number of RCC gravity dams due to their competitive cost and stability against overturning, sliding and thermal cracking as compared to embankment or arch dams. The use of the abbreviation "rollcrete" is proposed for roller compacted concrete according to soils Engineer's approach, "RCC" for that according to the concrete Engineer's approach and "RCD" for that according to the Japanese approach. Because of cost and a lack of suitable embankment materials, Saco Dam at Nova Olinda in Paraiba, Brazil, was redesigned and built with RCC. Successful actions were taken to control thermal cracking, including mix adjustments and addition of joints. A modified version of the original program 'THERM" from the University of California at Berkeley was used in the thermal analyses of Saco Dam (Quin, Rezende and Schrader, 1986). From the result of that analyses it was found that the maximum temperatures occurred around the middle elevation. They also showed that high temperature occurred rapidly within a few days from placement due to chemical hydration. The studies clearly showed the importance of minimizing cement content and volume of conventional concrete, so that thermal stresses and subsequent cracking in the dam were minimized. Thermal FEA analysis for 2-D model of the Urugua-í Dam in Argentina, was also studied. The procedure (Cervera, Oliver and Prato, 1999) performed suitable studies in order to establish the effect of some major variables of the layer-wise construction process of Urugua-í RCC Dam that had an influence in the temperature distribution and evolution, such as, placing temperature and the placing intervals. The results of the temperature and thermal stress evolutions inside the Hinata dam was compared and found to comply with those studies.

PROBLEM DESCRIPTION

Hinata dam was built at Kamaishi city of Iwate Prefecture situated in the northern part of Japan. The dam was a 56.5m high gravity structure of RCC above foundation with crest length 290m, crest width 5m, bottom length 15m, bottom width 30m, RCC volume 191,362/m^3, upstream face was vertical, downstream face with a slope of 1:0.75 (v:h). The dam geometry is shown in Fig. 2. The details are presented in Table 1. The upstream facing, spillway crest and the downstream facing were built with Conventional Portland Concrete (CPC) with cement content of 170 kg/m^3. The body of the dam was built with RCC90. There were two main transverse contraction joints each placed 53.5m away from the central transverse section. Facing concrete had contraction joints every 12m.

Table 1. Characteristics of Hinata Dam

Type of Dam	Concrete Gravity
Height	56.5m
Crest Length	290.0m
Slope Gradient	Upstream (Upward); Vertical Fillet (Upward) Slope Gradient 1:0.2 Downstream Slope Gradient 1:0. 75
Volume	240,000 m^3
Elevation of Base	112.0 m
Top Elevation	167.5 m
Design Flood Discharge	630 m^3/sec
Surcharge Water Level	164.5 m
Total Catchment Area	22.0 km^2
Water Stored Area	0.29 km^2
Total Volume Storage	5,700,000 m^3
Effective Water Storage	5,000,000 m^3
Flood Control Volume	4,9000,000 m^3
Volume of Sand	7,000,000 m^3
Water Level Elevation	136.5 m
Send Level Elevation	135. 4m

Approximate RCC composition

Portland cement 90 kg/m^3, Fly ash 34 kg/m^3, Water 147 kg/m^3, Fine Aggregate 802 kg/m^3, Coarse aggregate 1251 kg/m^3, Water percent by dry wt. 8.5%. Water was readjusted based on aggregate free moisture content before mix.

Dam Site Climate

Average minimum, maximum temperatures during winter and summer months were 2.5°C, 14°C and 16°C, 28°C respectively; the average annual temperature 13.5°C, and the humidity varied from 20% to 60%. The average global radiation energy for the winter and summer months were recorded as 2.60 and 3.95 kWh/m^2. Atmospheric temperature variation with time was recorded as shown in Fig. 3.

Material Properties Used For Hinata Dam

Material properties were taken according to Table 2. The entire body of the dam made with RCC90, except the foundation, was used for FEA analysis. For RCC90, coefficient of thermal expansion, $\beta=10^{-5}$ /°C, convection heat transfer coefficient, h_c=25.8 W m^2.°C, emissivety = 0.91, Young's modulus of elasticity, E=25 MPa, Poison's ratio = 0.17.

Table 2. Material properties for Hinata Dam

Property	RCC90	RCC120	CPC	Rock
ρ (kg/ m^3)	2350	2380	2450	2700
c (J/kg. ^{0}C)	0.21	0.22	0.22	0.21
k (W/m. ^{0}C)	0.88	0.89	0.89	1.00
w/c	1.00	0.80	0.50	-

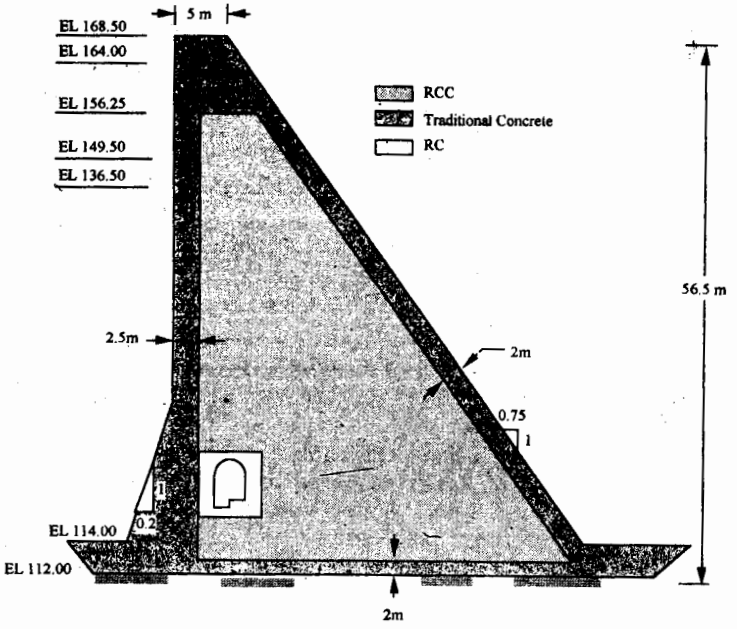

Fig 2. Gemetrical Configuration of Hinata Dam

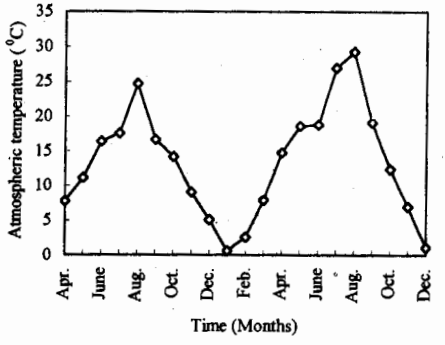

Fig 3. Monthly temperature variation of the ambient

Foundation

The 3.5m deep foundation was made by RCC 120 placements of 0.5m thickness with high cement content of 120 kg/m^3. Before the beginning of the foundation construction, about 1.5m deep bed of rock was built at the bottom.

MATHEMATICAL MODEL FOR THE FINITE ELEMENT

Thermal Relations

The problem was simplified by assuming some hypotheses without limiting it with too many restrictions. The temperature variations were taken in the range between 0°C and 50°C. Assuming the RCC as stationary, homogeneous, and isotropic material, the analysis was done. Heat generation due to early age chemical hydration of cement in RCC was taken into account. Half symmetry due to equal initial and boundary conditions was considered.

Governing Equation

The governing partial differential equation used for the three-dimensional transient heat conduction in Cartesian coordinate was:

$$\rho c \frac{\partial T}{\partial t} = [K]\nabla^2 T + \dot{Q}_K \qquad (1)$$

where, ρ = density, c = specific heat, T = T (x, y, z, t) = temperature, [K] = thermal conductivity matrix.

Initial Condition

Initial condition specified the initial distribution throughout the body. The initial condition associated with Eq. (4) was defined as

$$\lim_{t \to 0} T(P, t) = T_0(P) \qquad (2)$$

where, any point P = P(x, y, z)

Boundary Conditions

i) Prescribed temperature T^* acting over the surface:

The surface temperature of the boundaries was specific to be a function of space and time.

$$T(P, t \neq 0) = T^* \qquad (3)$$

where, T^* = Specified Temperature

ii) Prescribed heat flux acting over the surface:

$$\{q\}^T \{n\} = q_K \quad (4)$$

where, q_K = heat flux.

iii) Heat transfer from surface to ambient by convection was expressed by Newton's cooling law as:

$$\{q\}^T \{n\} = -h_c \{T_b - T\} \quad (5)$$

where, T_b = is the bulk temperature of surrounding atmosphere, T = surface temperature, h_c = heat transfer coefficient (assumed to be positive).

The convective coefficient h_c was influenced by wind velocity V. The following relationship was established [Froli, 1993] during the simulation of natural convective exchange for air-concrete interface

$h_c = 5.6+4.0V$ for $V<5$ m/s

$= 7.15V^{0.78}$ for $V \geq 5$ m/s

iv) Solar radiation absorbed by the dam surface was expressed as

$$\{q\}^T \{n\} = \alpha(I_d + I_i) \quad (6)$$

where α = absorptivity of the concrete surface, I_d = direct solar radiation, I_i = indirect (diffused) solar radiation.

The above equation for solar radiation contained complex variables such as hour of the day, the day of the year, the latitude and the altitude of the dam and the cloudiness of the sky. Its estimation involved laboratory procedure using pyranometer at the site of the dam considering the evolution during any day from which averaging was done over months.

The entire superficial heat transfer through exposed surface was expressed as an equivalent convection heat exchange between surface temperature T and the suitable fictitious temperature T_b^* which was termed as "equivalent atmospheric temperature" because it included both the effect of air temperature and heat from the sun (Saetta, Scotta and Vitaliani, 1995).

$$\{q\}^T \{n\} = h_c(T^*_b - T) \quad (7)$$

$$\text{with, } T_b^* = T_b + \frac{\alpha}{h_c}(I_d + I_i) \quad (8)$$

The specifications of the above boundary conditions in any combination over different problems of the body surface, together

with specification of the initial temperature distribution leaded to a unique formulation of the transient heat conduction problem. Heat generation due to hydration process was characterised by:

$$q''' = \rho c \frac{\partial \Omega}{\partial t} \tag{9}$$

where, $\Omega(t)$ was obtained from curve fitting on experimental data (Tu and Niu, 1988) and was expressed as:

$$\Omega(t) = 28.96\ (1-e^{-0.38t})\ ^{o}C \tag{10}$$

Thermoclastic Relation

Three hypotheses were assumed (Zeinkiewicz and Taylor, 1991) in order to evaluate the strees-strain conditions in the displacement field due to time-and space-variable thermal loads, as mentioned below:

(a) Temperature field was determined by taking into considerations, the effect of coupling of temperature and strain fields. Temperature field was always depended on deformation.

(b) Strains and displacement fields were infinitesimal: Their relationship was expressed as:

$$\{\varepsilon\} = \frac{1}{2}\left\{\dot{u}\right\} \tag{11}$$

where, $\left\{\dot{u}\right\}$ = derivative of displacement vector

(c) Material obeyed generalised Hook's law. This hypothesis evaluated material relationship for linear elastic materials. The stress was related to strains by:

$$\{\varepsilon\} = \{\varepsilon^{th}\} + [D]^{-1}\{\sigma\} \tag{12}$$

where, $\{\varepsilon\}$ = total (elastic plus thermal) strain vector,

$\{\varepsilon^{th}\}$ = thermal strain vector

where, β = coefficient of thermal expansion, $\Delta T = T - T_{ref}$, $T=T(P, t)$, T_{ref} = reference (initial strain-free) temperature, [D] = elasticity matrix, and $\{\sigma\}$ = stress vector

The thermal strains $\{\varepsilon^{th}\}$ occurred due to temperature-dependent thermal expansion. For isotropic material it was expressed as (Lewis, Morgan and Zeinkiewicz, 1981):

$\varepsilon^{th} = \delta_{kl} \cdot \beta \cdot (T - T_{ref})$ (13)

where, δ_{kl} = Kronecker delta = $\begin{cases} 1, & if, k = 1 \\ 0, & if, k \neq 1 \end{cases}$

Boundary conditions

The boundary of the solution domain was divided into the free portion and the bound portion so that,

$\{\sigma\}\{n\} = \{f\}$, on the free domain

where, $\{n\}$ = unit vector normal to the boundary surface, $\{f\}$= free-surface traction vector, and, $\{u\} = \{U\}$, on bound portion

where, $\{U\}$ = prescribed displacement vector on the bound surface.

Finite Element Formulation

After spatial discretization, the heat transfer equation (1) assumed the following form in terms of matrix notations:

$$[C_c]\frac{d\{T_c\}}{dt} + [K_e]\{T_e\} = \{Q_e\} \quad (14)$$

where, $[c_e] = \rho c \iiint \{N\}\{N\}^T \, dV$ = element specific heat matrix, where $\{N\} = \{N(x,y,z)\}$ = element shape function $\{T_e\} = \{T_e(t)\}$ = nodal temperature vector $[K_e]$ = element conductivity matrix = $\iiint [B]^T [K][B] dV + \iint h_c \{N\}\{N\}^T dS$ where, $[B] = \nabla\{N\}^T$; and $\{Q_e\}$ = $\iint \{N\} q'' dS + \iint T_b \cdot h_c \{N\} dS + \iiint q''' \{N\} dV$ = element convection surface heat flow vector.

Time Stepping Scheme

The Eq. (14) as integrated in the time domain, which leaded to the following algorithm for numerical solution (Zienkiewicz and Taylor, 991)

$$[C_e]\left\{\frac{T_e(t+\Delta t) - T(t)}{\Delta t}\right\} + [K_e]\{\omega T_e(t+\Delta t) + (1-\omega)T_e(t)\} = \omega Q_e(t+\Delta t) + (1-\omega)Q_e(t) \quad (15)$$

Where Δt = time step. For $0.5 \leq \omega \leq 1$ the algorithm was unconditionally stable, and for $\omega = 0.5$ the order of accuracy was 2 (Zeinkiewicz and Taylor, 1991)

PROCEDURE

Concreting of the the foundation began in August 1994 and was completed in March 1995. The foundation work was temporarily suspended in January and February of 1995 due to colder weather.

RCC placing for the body of the dam began in April 1995 and was completed in December 1996. It took approximately 20 months for the construction process to be completed.

The three-dimensional mesh represented the body of the dam from elevation 112 m to elevation 168.5 m. Foundation work was not included in the FEA model. The upstream facing, spillway crest and the downstream facing made with CPC, were assumed to be made of RCC90 to simplify the model, so that RCC90 was indicated simply by RCC. The computer program allowed the simulation of different stages of the actual player-wise construction process of the dam. 0.75m-compacted lift thickness was specified to achieve satisfactory density and strengths during compaction. Compaction was done to approximately 98% of the maximum density. Most of the RCC layers were placed at temperate weather. To minimize thermal insulation due to contact between layers and to eliminate potential seepage there from, about 12.75mm thick bonding mortar mix was mechanically placed between successive lifts. Freezing and thawing problems were successfully avoided by temporarily suspending the construction work for the months of January and February. However proper precautions were made for the possibility of freezing conditions.

Actual *in situ* temperature measurements were obtained by setting temperature sensors at different elevations. Temperature data were monitored on a routine basis for each RCC lift throughout its exposure. By using those temperature data in tabulated form, along with physical and thermal properties of RCC, the computer program used the thermal equations to predict the temperature and thermal stress development inside the body of the dam.

Half symmetry due to equal initial and boundary conditions about the central transverse section was considered during the analysis to reduce computer time. Convection loads were applied to the surfaces in contact with air. Initially the body of the dam was mashed by providing coupled-field 8-node, 3-D hexahedral elements with temperature and structural displacement as their degrees of freedom. The number of elements in the mesh was 5625 with total of 7296 nodes. In the vertical direction the FEA element depth was taken to be equal to the layer thickness used. The use of coupled-field elements for the body of the dam allowed, at first, to get the temperature distribution at different time. The stress distribution induced due to temperature effect was then obtained once the temperature field was known. Experimental solar radiation data were input as a tabulated form to the program. Solar radiations absorbed by the exposed surfaces were applied by providing superimposed 4-node, 3-D quadrilateral surface-effect speciality elements, SURF 152, over the exposed surfaces already meshed with SOLID5 elements that received radiation, SURF152 had got the temperature as its single degree of freedom. It was required by the ANSYS/Thermal

program to apply radiation loads separately after all the conduction and convection loads were applied. Thermal radiations liberated from the exposed dam surfaces to the ambient were very small and were neglected.

For placing temperatures, T_p, of RCC layers as compared to the ambient temperatures, $T_{amb.}$, at the time of placing, three different cases were considered: (1) $T_p = T_{amb.} + 3^{\circ}C$ (no pre-cooling, reference case); (2) $T_p = T_{amb.}$ (mild pre-cooling); and (3) $T_p = T_{amb.} - 3^{\circ}C$ (intense pre-cooling). Some pre-cooling was effective especially during the summer season due to the low thermal conductivity of RCC and to speed up the placing process, as this would reduce the time that a newly placed lift was exposed to the ambient temperature. For the reference simulation case the placing temperature of each lift was taken as equal to the ambient temperature corresponding to their placing date plus $3^{\circ}C$. This increase in placing temperature was assumed to be due to the stocking conditions and the manipulation operations done during the production process of RCC.

In the FEA program, initially the lowest block of 3 m, consisting of 4 layers, just above the foundation was analysed. The meshes corresponding to the next and every 3 m high RCC blocks were progressively added, at the times corresponding to their respective placing in the dam, to the total depth of the dam already analyzed at the bottom. Placing of the RCC layers were simulated by assuming a placing interval range of 5 to 7 days, therefore, blocks of 4 layers were added one at a time, within the range of 20 to 28 days. Total of 75 layers with 0.75 m height, except the topmost layer that was 1 m high, were placed to complete the body of the dam.

The time step used in FEA method during construction of the dam was 12 hours, so that once a block was added, within the range of 40 to 56 time steps passed before a new block was placed above. During this time the temperature of the newly placed block varied according to the ambient temperature on top and the temperature of RCC already placed below. The RCC blocks reached a significant hydration and aging degree before another block was placed on top. The maximum range of 18 hours and minimum of 6 hours of time stepping provided for automatic sub-stepping to accurately integrate the evolution of the aging degree. Minimum time step would be used during early-age hydration.

RESULTS AND DISCUSSIONS

The contour plots for the development of temperature into the dam mass at four different stages of construction with elevations of 121 m (Stage-1, June 1995), 139 m (Stage-II, November 1995), 154 m (Stage-III, April 1996), and 168.5m (Stage-IV, December 1996) were observed as shown in Fig. 4 (a), (b), (c) and (d), respectively. Only the central transverse section (plane of half symmetry) was

noted for the isotherms. The other surfaces of the 3-D body were not shown because they retained the same temperatures as the ambient. The temperature development in October 1997 and October 1998, after the completion of the dam, were noted as shown in Fig. 5 (a) and (b). The graphical representation of temperature development for interior points corresponding to lifts of 3 m block placed with 1-month intervals between them were obtained as shown in Fig. 6, where the elevations corresponding to placing months were taken as follows: (1) 115m, (2) 118m, (3) 121m, (4) 124m, (5) 127m, (6) 130m, (7) 133m, (8) 136m, (9) 139m, (10) 142m, (11) 145m, (12) 148m, (13) 151m, (14) 154m, (15) 157m, (16) 160m, (17) 163m, and (18) 166m. Placement of RCC layers for the body of the dam started in April 1995, 3 months after completion of the foundation of up to 112m elevations. The average placing temperature of the layers just below 115m elevation of the dam body became 10.5°C after adding 3°C with the ambient temperature in April 1995. The layers just below the top surface (121m) in stage-I were placed at higher ambient temperature in June 1995 and their placing temperatures were around 19°C. From Fig. 6, the peak temperature for elevations 115m and 121m, was found to be about 17°C and 24°C, respectively. These temperatures complied with the contour plots, which showed that the temperature at the bottom of stage-I was low and at the top it was higher. Similarly in stage-II the placing temperature at the top, just below 139m elevation, was around 13°C with peak of about 17°C and at the middle, near 127m elevations, it was around 24°C with peak of about 27.79°C. In stage-III, the upper layers, just below 154m elevation, were placed at around 19°C with peak of about 26°C and the layers at the middle, near 143m were placed at around 8°C with peak of about 14°C. So that the contour plots in stage-III are separated into two distinct upper and lower high temperature regions. In stage-IV, the layers just below 166m were placed at about 21°C in September with a peak of about 27°C. On the other hand, the layers, just below 163m elevations, were placed at about 31°C with a peak of about 35°C, so that the two distinct upper and lower high temperature region remained. The layers above 121m, of the dam body experienced very slow increase in temperature, because of the greater depths of those layers. The layers placed below 121m elevation showed decreasing temperature, since they lost temperature through foundation rock. In Fig. 6, a small amount of temperature drops of the lifts placed between 139m and 148m elevations were observed because of the placement break during January and February due to colder weather. Form Fig. 5 (a) and (b), it was clear that the temperature in the interior of the dam decreased progressively as the heat generated during the hydration process was released through the upstream and downstream faces of the environment and, to a minor extent, to the foundation rock. The cooling was faster in the upper part of the dam, where the surface-to-

volume ratio was higher. The upper 'hot spot' had completely disappeared after 20 months (October 1998) from the end of construction. From this evolutionary temperature distribution, it was predicted that after about 5 years from the date of completion of the dam, the body of the dam would then be in a thermally stable regime, subjected only to the cyclic seasonal oscillations.

Fig 4(a). Temperature development after completing 121m elevation (June '95)

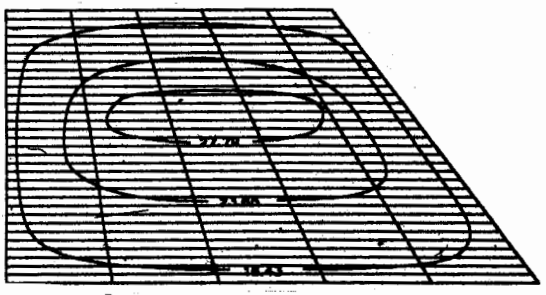

Fig 4(b). Temperature development after completing 139m elevation (November '95)

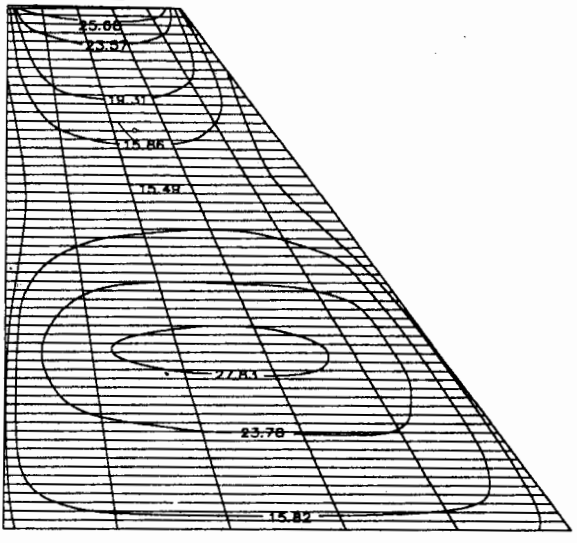

Fig 4(c). Temperature development after completing 154m elevation (April '96)

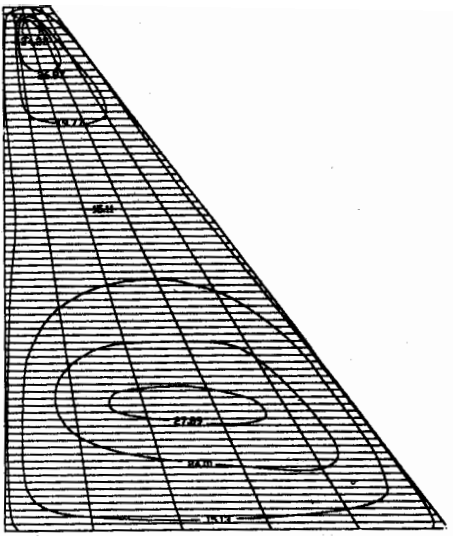

Fig 4(d). Temperature development after completing 168m elevation (December '96)

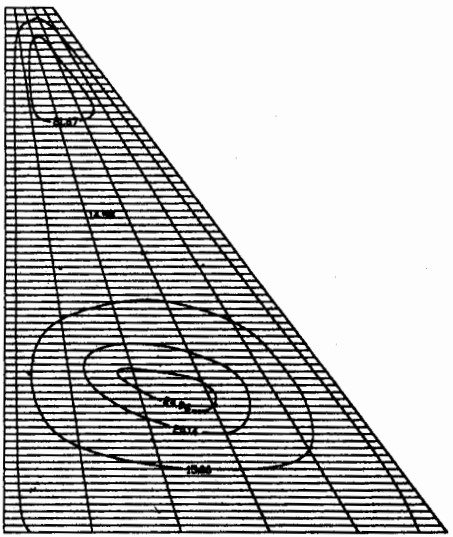

Fig 5(a). Temperature development in October '97, 10 months after completion of dam

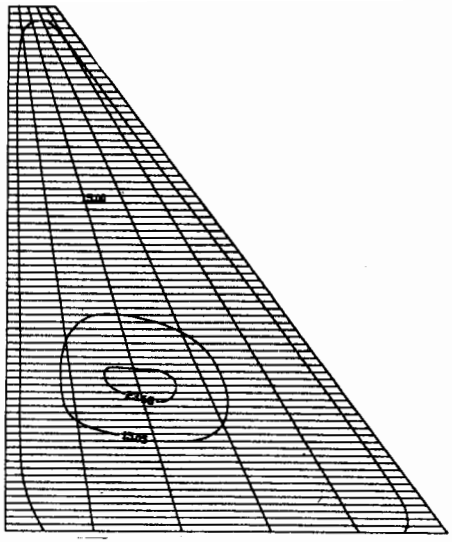

Fig 5(b). Temperature development in October '98, 22 months after completion of dam

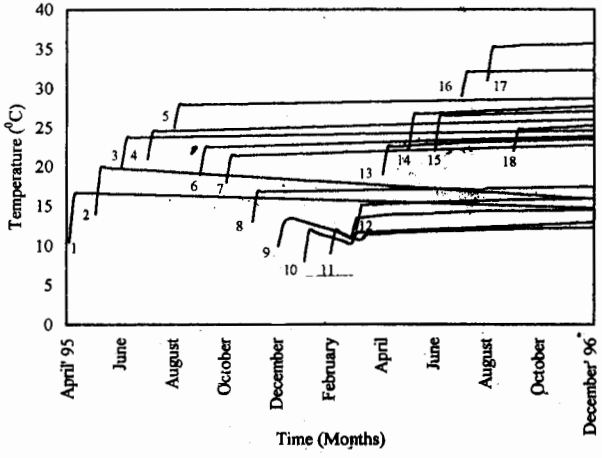

Fig 6. Temperature changes during layer-wise construction of Hinata Dam

During summer, the average placing temperature for the lifts was about 25°C, and it was maintained by using mix of cooling water of 6°C with stones of about 30°C and cement of about 31°C. During

winter, the average placing temperature for the lifts was maintained at about 12°C in order to comply with the ambient to avoid excessive temperature gradients. Maintaining this low placing temperature in winter was facilitated by very low temperature of stones, about 5°C, although mixing water used was about 40°C supplied from boiler and cement about 25°C. The temperature of RCC placed was such that the net temperature rise resulting from hydration of cement and exposure to the ambient would not produce a peak temperature that could exceed the final stable temperature by more than the allowable temperature drop of 10°C. Moreover certain precautions were taken during construction by providing plastic membrane insulation temporarily over the exposed surfaces to prevent heat loss to the ambient by evaporation, conduction and convection, until the temperature differential was reduced to about 10°C.

When the RCC was not pre-cooled (reference case) due to temperate weather at the dam site, the principal means to reduce the temperature rise was the flow of heat from the top exposed surface to the atmosphere. For the reference case, the optimum RCC layer thickness for lifts was established by laboratory procedures at 0.75m. With this thickness the temperature rise at the bottom of the lift was found to be adiabatic for the first 2 days after placement and the maximum temperature was reached in the next 3 to 5 days as shown in Fig. 7. The temperature rise started to minimize thereafter.

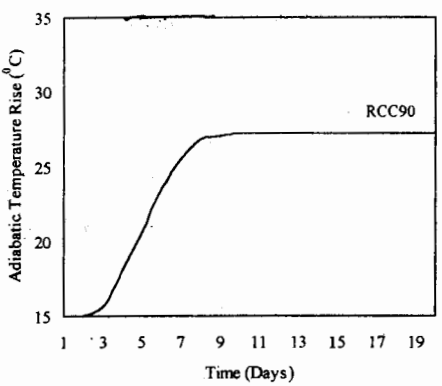

Fig 7. Adiabatic temperature rise in RCC

The computed temperature development (solid line) at elevation 124m was compared with sensor data (dots) as shown in Fig. 8. The agreement between the FEA model predictions and actual sensor temperatures was remarkable.

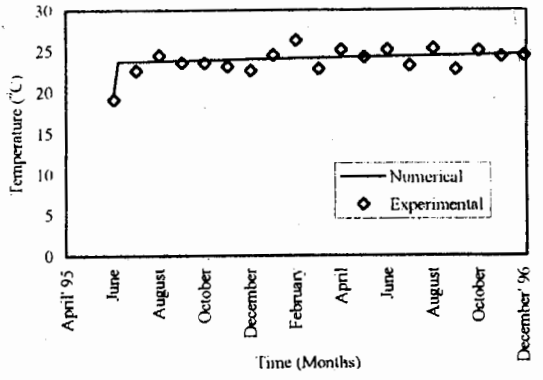

Fig 8. Comparison between numerical and experimental temperatures at 124m elevation

During freezing and thawing either the cement paste or the aggregate or both could be damaged by dilation. During dilation, stresses could exceed the proportional limit, which would cause permanent enlargement or actual disintegration. Dilation and associated stresses were belived to be due to hydraulic pressure generated when growing ice crystals displace unfrozen water and cause it to flow against resistance to unfrozen portions of the dam mass. Entrained air inside concrete served as reservoirs for the relief of pressure developed within the freezing concrete and thus relive or avoid the high tensile stresses that could lead to failure. The RCC of the dam contained pores in all its constituents and thus some entrapped air inside pores, usually between 0.5 and 1.5%, which was relatively ineffective in increasing resistance to freezing and thawing. Excess of 4 to 6% air was purposefully entrained in RCC by decreasing the maximum size of the aggregate to about 3.75cm, which greatly increased resistance to freezing and thawing. Air entrainment affected the properties of freshly mixed and hardened concrete. Freshly mixed air entrained concrete was more plastic and workable, whereas, hardened concrete containing entrained air was more uniform, had less absorption and permeability, and was more resistant to the action of freezing and thawing. However, entrained air was not allowed to exceed 10% of the RCC mix because each percent of entrained air in concrete could result in about 5% decrease in compressive strength of RCC. Due to cold weather condition during winter, RCC layers had to be placed at low temperatures but of course above freezing temperature, and not less than 4.5°C. It developed higher ultimate strength and greater durability than similar RCC layers placed at higher temperature. Under colder conditions the temperatures of the freshly placed RCC

were obtained by preheating the mixing water up to maximum of 60°C.

Very high temperature conditions, on other hand, could produce problems such as acceleration of RCC layer setting rate, increase evaporation of mixing water which could increase the required amount of mixing water, reduce ultimate strength and thus increase the tendency to crack. Cooling the ingredients up to 4°C, minimized the undesirable effects of hot weather.

No galvanized reinforcing steel was used with RCC, which was more susceptible to corrosion. Since some non-ferrous metals were used in contact with RCC, the possibility of corrosion contact had to be considered. Aluminium was used for coils, pipelines, and linings for concrete vats; copper was used for diaphragms in joints; lead was used for cable sheathing and for lining tanks. Aluminium was protected with asphalt coating. Copper was almost inactive to caustic alkalis either in fresh or in hardened concrete. Lead in contact with fresh concrete could react with calcium hydroxide and thus could develop corrosion. Protective coating with asphalt or varnish, or pitch was provided to protect corrosion due to lead.

Thermally induced stress (principal) distribution in December 1996 and October 1997 was found as Fig. 9 (a) and (b). The 3-D mesh showed the evolution of thermal stress for the central transverse section and the exposed surfaces of the body of the dam. As the RCC started to warm because of the release of the hydration heat and the heat flux coming from the surrounding RCC, the stress at first mainly became compressive. This lasted until the RCC began to cool after the hydration process was finished, and the heat in the dam body was released toward the ambient through the upstream and downstream faces and the foundation rock. However, up to October 1997 it was found that there was still compressive stress in the core of the dam body. It was due to the greater distance of the RCC in core from the exposed surfaces. As the temperature dropped, the longitudinal stress in RCC turned progressively from compression to tension. This phenomenon was faster for the upper elevations, because of higher surface-to-volume ratio. However, the upstream and downstream faces and the bottom lifts also went into tension very quickly because of the loss heat toward the ambient and foundation rock.

Minimum structural criteria established for the RCC mix design included: Unit weight: 2.45 g/cm^3, compressive strength: 20.8 MPa at 365 days, Static tensile strength: 1.7 MPa at 365 days, dynamic tensile strength: 2.4 MPa at 365 days. The resulting stress conditions obtained from analysis as compared to the established value showed that the maximum thermal stresses inside the dam were well within the safety limit to avoid potential cracks.

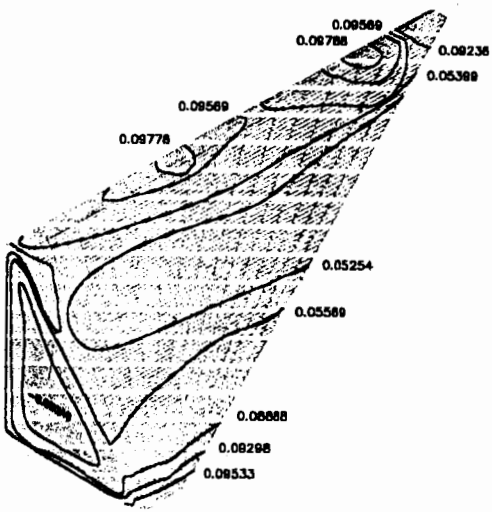

Fig 9(a). Stress distribution after construction (October '97)

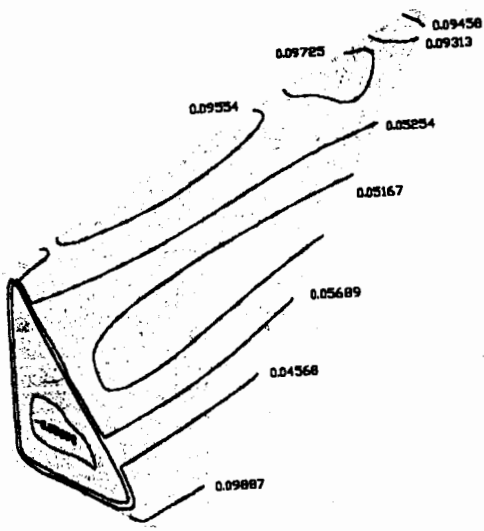

Fig 9(b). Stress distribution after construction (December '97s)

CONCLUSION

Study was undertaken at the northern part of Japan with temperate weather condition that provided with satisfactory working condition to avoid critical factors such as potential heat gain or loss through exposed surfaces of RCC layers. The peak temperatures of RCC did not exceed the final temperature of the RCC mass by more than 10°C. Sufficient precautions should be taken for hot weather.

The thermal analysis procedure included consideration of heat generation due to hydration, conduction and solar radiation, as influenced by environmental factors such as ambient temperature. The stress deformation analysis procedure included consideration of the temperature-induced and elastic effects.

The FEA procedure was found to be effective and of practical applicability in predicting the stress level induced by thermal variable loads in RCC structures. Although this paper demonstrated a realistic simulation to qualitatively assess the field construction conditions by the FEA program, it was believed that further enhancement were needed to include factors such as the non-linearity of the interaction between temperature and stress-strain fields, time-dependent creep effects, and material non-linearity, shrinkage, and fracture properties of early age RCC.

REFERENCES

Cervera, M., Oliver, J. and Prato, T. (2000), "Simulation of Constructin of RCC Dams", Journal of Structural Engineering (ASCE), September 2000, Vol. 126, No. 9, 1053~1070.

Froli, M. and Hariga, N. (1993), "La risposta termica per effetti ambient dei ponti in c.a. e c.a.p." Proceddings of '93 Giornate A.I.C.A.P. Pisa, AICAP, Rome, Italy, 161 ~ 170.

Quin, J. T., Rezende, S.P. and Schrader, E.K. (1988), "Saco Dam – South America's First RCC Dam", Proceedings of '88 ASCE Conference, San Diego, California, U.S.A., Feb 29-Mar 2.

Saetta, A., Scotta, R. and Vitaliani, R. (1995), "Stress Analysis of Concrete Structures Subjected to Variable Thermal Loads", J. Struct. Eng., Vol. 121, No. 3, ASCE, 446-457.

Tu,C. L., and Niu, Y.Z. (1988). Thermomechanical test of Dongjiang arch dam concrete, Tech. Rep., Research Centre of Structure and Materials, Mid-South Design Inst. For Hydroelectric Projects, Changsha, Human, China.

Zienkiewicz., O.C. and Taylor, R. L. (1991), The Finite Element Method Vol. 1-2. McGraw Hill Book Co., Inc., New York, USA.

NOTATION

α	Absorptivity of concrete surface
c	Specific heat
$[D]$	Elasticity matrix
E	Young's modulus of elasticity
f	Free-surface traction
h_c	Convection heat transfer coefficient
I_d	Direct solar radiation
I_i	Indirect solar radiation
$[K]$	Thermal conductivity matrix
N	Element shape function
$\{n\}$	Unit vector normal to the boundary
P	Any point, P(x, y, z)
T_b	Bulk temperature of ambient
T	Temperature, T (x, y, z_t)
t	Time
q''	Heat flux per unit area
q'''	Heat generation rate per unit volume
U	Prescribed displacement
u	Displacement
V	Wind velocity
β	Coefficient of thermal expansion
δ_{kl}	Kronecker delta
ε	Total strain
ε^{th}	Thermal Strain
ρ	Density
σ	Stress
Ω	= Ω (t) = temperature